

Coarse Segmentation With GDD Clustering Using Color and Spatial Data

EMRE GÜNGÖR¹, AND AHMET ÖZMEN², (Member, IEEE)

¹Department of Computer Engineering, Alanya Hamdullah Emin Pasa University, 07400 Antalya, Turkey

²Software Engineering Department, Sakarya University, 54187 Sakarya, Turkey

Corresponding author: Emre Güngör (emre.gungor@ahep.edu.tr)

ABSTRACT Segmentation is a challenging and important task in image processing while developing vision based decision support systems. Color and brightness are widely used properties for extracting segments, however color information usage becomes more crucial for better region distinction, especially on outdoor scenes where brightness value makes segmentation difficult. In this study, a novel segmentation algorithm which incorporates downscaling and clustering methods has been developed to find consistent coarse regions in a given input image. The new method does not require external parameters and produces consistent segmentation results on different runs. In the algorithm, two intermediate segmentation results are obtained by feeding dissimilar downscaled image information to GDD (Gaussian Density Distance) clustering method. The outputs form two different perspectives from the same image: one shows global level color distinction, and the other shows spatial color similarity information. A merging process of these two outputs is implemented to improve the final segmentation. During the study, an experimental framework is designed for analysis of the proposed approach and its evaluation. The method is extensively tested using benchmark images. Some of the selected results are presented in the paper along with a comparative study with well-known segmentation algorithms.

INDEX TERMS Coarse segmentation, color segmentation, GDD clustering, image downscaling, spatial segmentation, parallel image segmentation.

I. INTRODUCTION

Advances in technology have made vision computing applications available for more areas such as automotive, security, decision support systems and many others. Image segmentation is one of the most studied subject in the area which is based on grouping of pixels with their properties such as similarity, proximity, continuity, symmetry, parallelism, closure and familiarity [1]. A simple segmentation method is thresholding, which can be done as grouping the pixels against a certain threshold value of brightness or color [2]. Other well-known and widely used image segmentation algorithms are implemented by using histogram, edge detection, region-growing and clustering [3]–[6]. Perceptual weights are studied in segmentation to improve region-based image segmentation using pooling strategies [7]. Recently, neural network based semantic segmentation approaches have also become widespread [8]–[11]. Different methods may

produce slightly different segmentation outputs for the same image, which is not a flaw because application requirements usually determine the expected details. For example, while it is important to find the number of people and their locations in the image for one application, locating a tumor and its size is more important in medical area, which may require very specific segmentation methods.

Some of these techniques mentioned above have been developed for mono-chrome images, and there are studies to extend them for color images. Since color carries far more information relative to gray-scale, it can be used for different approaches during segmentation [12]. Color segmentation is also more robust against brightness of input images, and it produces better output with irregular illumination changes [13]. However, sharp changes on the light sources may cause error on output.

In this paper, coarse segmentation algorithm that finds regions based on color and spatial data from downscaled images using Gaussian Density Distance (GDD) clustering is presented. In this new approach, multiple segmentation

The associate editor coordinating the review of this manuscript and approving it for publication was Noor Zaman¹.

processes are run in parallel and composed to find more refined results. This approach does not require any special parameters a priori and resulting segments does not change at different runs. Two different approaches about feature processing by downscaling are implemented in the algorithm to improve the success rate. These approaches are independent from each other and produce slightly different segmentation outputs using the clustering method. The new algorithm is tested with several benchmark images and the results are compared with well well-known color segmentation algorithms. The results are comparatively good despite the presence of similar color regions, noisy images or textures.

A brief outline of remaining parts of the paper is as follows: In Section II, a summary of related literature is presented. In Section III, the algorithm, data structures and computation flow are presented in details. In Section IV experimental setup with image database and comparison metrics are explained. In Section V, comments and discussions about the results are presented.

II. RELATED WORK

Many color segmentation algorithms are presented in the literature and they are used for various purposes. The following sub-sections explain some well known image segmentation methods, supplemental approaches and assisting tools in detail.

A. CLUSTERING BASED SEGMENTATION

Clustering based segmentation methods vary from each other based on the image properties. These methods usually use histograms, pixel location information or color information to form clusters and segments [6]. For example, different color spaces and local histogram information are used by k-means clustering to combine several segmentation maps associated to simpler partition models to achieve more reliable and accurate segmentation [14].

However, clustering methods generally require prior parameters which affect the segmentation outcome greatly. In order to achieve the best result optimal parameters are needed, and many segmentation studies therefore use estimation methods to find the best possible parameters. In a study for example, meanshift method is used to find convergence points as cluster numbers and then k-means is used to find the clusters and segments [15]. Gaussian Density Distance (GDD) clustering method on the other hand does not require any prior parameters [16]. GDD finds geometric relations with density properties and connects all similarities unlike the other clustering methods. There are other statistical methods that perform unsupervised image segmentation using Gaussian kernel [17].

The meanshift method also performs clustering without parameterization by finding the maximum points of densities over the space and is frequently used in clustering analysis and image processing areas [18]. Meanshift filtering is used to detect the modes of every super pixel in spatial domain and range domain for salient object detection [19]. Meanshift

can also be used in conjunction with evaluational algorithm to tackle under and over segmentation problems effectively [20]. Unlike other clustering methods, the meanshift method shows better performance in image segmentation than global cluster number or threshold detection methods because it generates the cluster number based on the density center estimation. The advantage of meanshift method is that applications do not need a cluster count because it automatically estimates the local maxima in dense regions. Unlike the meanshift method, the GDD clustering method completes the clustering according to the ratios of the intensities and distances of the given inputs, not the peak of the intensities.

B. SEMANTIC SEGMENTATION

Semantic segmentation is usually implemented by neural networks and they use more information besides color, pattern, shapes through training provided by the input data set. The network is trained against the region of interest by given pre-defined segments, and then it classifies the remaining inputs based on the learned knowledge. One of the important studies in the field, for example, can separate regions based on the context using pyramid scene parsing network (PSPNet) [8]. A segmentation using with lightweight depth wise convolution method is developed in another study for mobile devices. This study aims to improve the performance of a segmentation task for devices that have limited amount of resources such as CPU, RAM etc [9]. There are also other semantic segmentation studies that use neural networks; for example Goggle uses atrous convolution technique to control the resolution at which feature responses are computed within “Deep Convolutional Neural Networks” (DeepLabv3) [11]. DeepLabv3 is also used in another study as a base, and its output is improved by using a special decoder to select best parts to refine the segmentation results [10].

C. OTHER CLASSICAL SEGMENTATION METHODS

1) THRESHOLD BASED SEGMENTATION

Thresholding is a broad term which can encompass all of the segmentation methods since some sort of reference value is required in the end for filtering un-interested parts. There are many different and complex segmentation approaches in literature developed mostly because of application requirements. The thresholding method is preferred because it is the simplest and easiest to implement among them. There are several variants of thresholding: fixed, adaptive, multi-level and seed based [2], [21].

The fixed threshold approach is usually implemented by applying a constant threshold value to pixel level information of the image. If the information, e.g. brightness value of a pixel, is greater than a threshold than the pixel is labeled to a class, otherwise it is filtered. The main problem of this approach is to find an optimal threshold value. A threshold estimation may be beneficial to obtain a desired segmentation output. For example, the threshold can be estimated based on the brightness histogram of the image. This method is simple

and quite successful in light objects on a dark background. Although shadow and light conditions over the image are challenging problem for most approaches, fixed threshold methods produce more erroneous results comparing to the others.

Seed based thresholds are generally identifies a band of thresholds each of which signify a marked area to find segments [22]. In this technique, a threshold is calculated for each region and the resulting threshold values are put together (interpolated) to form a thresholding surface for the entire image. A pitfall for seed based threshold approach is that real-life images are not consistent with the light and the texture compositions. Hence, using predefined variables over some specific areas sometimes result in errors [23], [24].

2) WATERSHED SEGMENTATION

Watershed which inspired by water flooding of geographic surfaces and interpreting to image segmentation is one of the well known segmentation approaches [25]. Watershed algorithm generally finds distinctions by flooding low intensity areas and when two floods intersect region boundaries are created. In this algorithm, the points where flooding begins become important; hence, selection of these points affect resulting segments greatly.

3) REGION GROWING SEGMENTATION

Region growing is one of the simplest method on segmentation which uses spatial information of image pixels. The method needs some parameters such as: an initial seed for start up point and gradual change information to determine boundaries of segments. Region growing approach looks for neighbor pixels around the seed and compares their properties with the seed point information. If gradual changes stay in the limits then the inspected pixel is included to the segment. Since seed properties define the region boundaries and scope of the segment, seed selection becomes very important. Even though parameter requirement is a disadvantage of the approach, several seed selection methods and comparative studies can be found in the literature [4], [5], [26].

Advantages of region growing method are that it has good success rate when the seed is selected correctly and easy to understand and implement. However, it is sensitive to noise and sudden changes in segments, hence light conditions also become important for segmentation. Similarities may cause over-segmentation at either small portion of edges or similar connected attributes. It is also susceptible to homogeneity, highly deviated regions, shadow or lightness can effect results greatly and can cause both over-segmentation or non-complete segmented areas [27].

4) GRAPH BASED SEGMENTATION

Normalized Cut (N-cut) algorithm is a graph based segmentation method which can be described as clustering on graphs. In general, N-cut provides the grouping of graph nodes by performing a normalized cut based on the total relative to all other nodes in a set of nodes examined, instead of the

minimum or maximum cut points on weighted graphs. Since the problem becomes NP time complex, the approximate result is obtained by solving eigenvalues [28]. The N-cut method basically divides the graph into two parts; however when applied recursively, segmentation algorithms can be used to find multiple regions. There are many improvement studies about graph based segmentation algorithms in literature [29], [30].

D. SUPPLEMENTAL APPROACHES AND ASSISTING TOOLS FOR IMAGE SEGMENTATION

1) USAGE OF EDGES

Contour based algorithms can also be categorized with the ones that use edge information to identify segments in images [4], [24]. However, since edge information is generally extracted using threshold on gray level image, edge information is often does not give fully contour of segments. Partial edge information can be used as clue for segmentation methods, however, false edge information will negatively affect the results especially on color segmentation. Even though intensity values are similar, the colors of the pixels can be different which may cause failures when the edges are extracted from gray level.

2) USAGE OF HISTOGRAM AND COLOR SPACES

Histogram transfers intensity values into frequencies which gives the brightness distribution of whole image when gray levels are used [3]. Similarly, when HSV histograms are considered for segmentation, it becomes an equivalent task that uses color instead of brightness. A color image holds more information on its pixels, hence more detailed information becomes available for segmentation. A drawback of the histogram approach, it provides a global information about the image but loses locational information of pixels which is also important in segmentation. When target images do not contain so much local changes, then histogram based segmentation algorithms performs well.

Segmentation using histogram and color information without spatial information usually fails due to disregarded texture composition and color density on whole image. For example, when low and high intensity green color exist on a leaf of a flower, high and low intensities will be segmented separately because of missing locational information even though they belong to the same area. As a result, histogram, color-space and intensity data all provide important information for segmentation. Histogram and color-space data of an image especially help determining the coverage area of a specific color region or intensity value.

III. PROPOSED APPROACH

In this work, a coarse segmentation algorithm has been developed that runs without any input parameters and produces consistent outputs for repetitive runs. The general flow diagram of the segmentation algorithm is shown in Figure 1. Hue-Saturation-Value (HSV) color representation model was

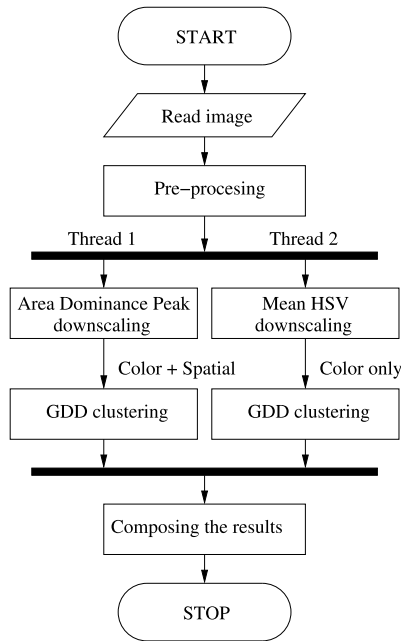


FIGURE 1. Flow chart of the proposed segmentation algorithm.

preferred in the calculations, however other well known color models could also be used in the algorithm. Hence, whenever required, RGB color values are converted to HSV space at the pre-processing stage.

As an intrinsic property, whole original image is downscaled by two different methods which are explained below. Downscaled sampling is inspired by rod/cone ratio in the human eye where human eye has less color receptors than brightness [31]. For the sake of segmentation speed and color region differentiation 1200 samples are taken from input images throughout the study, which is defined as an adaptive constant intrinsic property. As a generalized solution, different aspect ratios can be computed automatically needless of any external parameters.

A. AREA DOMINANCE PEAK (ADP) AND MEAN-HSV COLOR DOWNSCALING APPROACHES

The original input image is downscaled by two different approaches in two separate threads, and the downscaled images are then fed to the GDD clustering method for segmentation. After the clustering, the results are combined at the last phase of the algorithm to obtain the final output. Since the threads have independent tasks, they can run concurrently at different cores of any typical computer. In these methods, a pixel is represented as $\vec{P}(H, S, V)$ in color space, and $\vec{P}(x, y)$ in spatial space respectively.

1) AREA DOMINANCE PEAK (ADP) DOWNSCALING

A new method has been developed for finding the most dominant color in a block, called “Area Dominance Peak (ADP)” algorithm. Main motivation behind the ADP algorithm is to find the best representative color for a block. A representative

pixel selected using statistical calculations to express high probable dominant region in HSV color space in a block.

In the algorithm, an input image is scaled-down with a ratio of 1/8 first, and then, it is scaled-up back to the original size. This operation is used to eliminate recessive features, and to extract the dominant color regions. Then, the pixel differences are taken in the color space between the original and re-scaled images using the Equation 1, and the results are put into an array called \vec{C}_p .

$$\vec{C}_p = \vec{P}(H, S, V) - \vec{P}_{re-scaled}(H, S, V) \quad (1)$$

where $\vec{P}(H, S, V)$ and $\vec{P}_{re-scaled}(H, S, V)$ represent pixels in the original and the re-scaled image. The Gaussian Mixture Model (GMM) is used to find the color difference distribution considering the spatial information of each pixel. As it is shown in Equation 2, the pixel Gaussian distributions are multiplied by weights to propagate color information, and then they are accumulated to find the representative pixel in a block.

$$f_{sum}(\vec{P}(x, y)|w, \mu, s) = w_1 f_m(P_1(x, y)|\mu, s) + w_2 f_m(P_2(x, y)|\mu, s) + \dots + w_k f_m(P_k(x, y)|\mu, s) \quad (2)$$

where μ is mean, $s = \sigma/\sqrt{k}$ standard error of the mean, k is total pixel count in a block, and σ is the variance of the block pixel data. The weights (w_i) are calculated by an inverse impact factor (distance change on HSV color space) of scale-space operation where the maximum changes are getting the minimum weights, and vice versa (see Equation 3).

$$w_i = 1 - \frac{\|\vec{C}_{p_i}\|}{\sum_{j=1}^k \|\vec{C}_{p_j}\|} \quad (3)$$

$$\sum_{i=1}^k w_i = 1 \quad (4)$$

where k is the total pixel count in a block. Gaussian distributions for each pixel in the block (f_m) can be described as follows:

$$f_m(\vec{P}(x, y)|\mu, s) = A \cdot \exp\left(-\left(\frac{(x - x_0)^2}{2(\sqrt{\mu_x s_x}/2\pi)^2} + \frac{(y - y_0)^2}{2(\sqrt{\mu_y s_y}/2\pi)^2}\right)\right) \quad (5)$$

As a probabilistic distribution A can be calculated where integral of f_m function equal to 1. Since Equation 7 uses the maximum argument, the coefficient A may not be used in the calculations. x_0 and y_0 represent the reference point in the spatial domain. The simplified version of Equation 2 can be written as in Equation 6:

$$f_{sum}(\vec{P}(x, y)|w, \mu, s) = \sum_{i=1}^k w_i f_m(\vec{P}_i(x, y)|\mu, s) \quad (6)$$

The color of a block is determined by locating a representative pixel in the block using the distribution obtained by Equation 6. This representative pixel lies at the maximum point of the distribution (see Equation 7).

$$[H, S, V]_{block} = [H, S, V]_{pixel_with_max(f_{sum})} \quad (7)$$

After ADP algorithm, the block color information along with its spatial information are forwarded to the GDD clustering. This process protects color information instead of spatial information when resolution is reduced. As a result even though edge information may not be transferred, however correct color data can be accessed for each region. So, tradeoff in downscaling in ADP is in favor of the color rather than the shape.

2) TAKING THE MEAN OF HSV DOWNSCALING

Mean-HSV downscaling is a simple mean operation over a block in the original image done for each downscaled pixel. This approach is used for general estimation of color regions on global and block level.

3) COMPOSING THE RESULTS

After both threads finish the clustering, an intersection data is calculated using the two threads outcome. The final segmentation includes strong pixel elements where they exist at two output sets, and the weak elements where they only show up at one set. The weak elements are generally outliers that appear at segment borders.

As an example, Figure 2 shows the original image (513 × 383 pixel), the intermediate images of the threads and the final output. ADP and mean-HSV downscaling are followed by GDD clustering, and these two threads yield

different outputs. The variances between these two outputs can be seen in Figure 2.b-c.

B. GAUSSIAN DENSITY DISTANCE (GDD) CLUSTERING

The main objective of the GDD clustering algorithm is that it does not require any input parameters and produces consistent outputs. It also finds cluster members adaptively within different density areas [16]. Meanshift algorithm also clusters data without requiring any parameters. However fundamental differences such as peak estimation and random cluster position nature of meanshift makes GDD method more suitable for the task.

IV. EXPERIMENTAL SETUP

The proposed segmentation algorithm is implemented using MATLAB by Math-Works [32]. It is run on a computer with 32 GByte RAM and Intel i7-2600K quad-core 64 bit CPU 3.40 GHz. The new segmentation algorithm has been tested with many different images, and output of 11 different benchmark images from “The Berkeley Segmentation Dataset and Benchmark” has been presented in this paper [33]. Most of the presented images are 321 × 481 pixel in resolution, and their segmentation took approximately 8-10 seconds each using the proposed algorithm without any optimizations.

Table 1 shows comparison results with proposed method and well-known classical segmentation algorithms such as k-means color, k-means spatial, meanshift color and meanshift spatial [34], [35]. The presented approach is also compared with semantic image segmentation methods that use pre-trained neural network models such as “model 1-4” [8]–[10]. These networks are trained using with ADE20k, Cityscapes, PascalVOC datasets. The ground truth data came with the image data-set, and the input parameter for k-means method was entered as segment count from the ground truth table [33].

As classification and clustering have different origins, their comparison may lead to unneeded disputes as one does not use readily available data. Nevertheless applications wise comparison may be helpful for general case scenario where user may need to select a methodology based on different criterias such as available training data, timing constraints, input image resolution or expandability of the segmentation system.

Evaluation has been performed using the Purity, Conditional Purity, F-measure (F-1 and F-2) and Normalized Mutual Information (NMI), Intersection over Union (IoU/Jaccard Index) metrics and the results are presented in Table 1. Purity is a simple and transparent evaluation measure for clustering methods [36]. Each segment is assigned to the class which is most frequent in the segment, and then the accuracy of this assignment is measured by counting the number of correctly assigned elements and dividing by N (see Equation 8).

$$purity(\Omega, \mathbb{C}) = \frac{1}{N} \sum_k \max_j |\omega_k \cap c_j| \times 100 \quad (8)$$

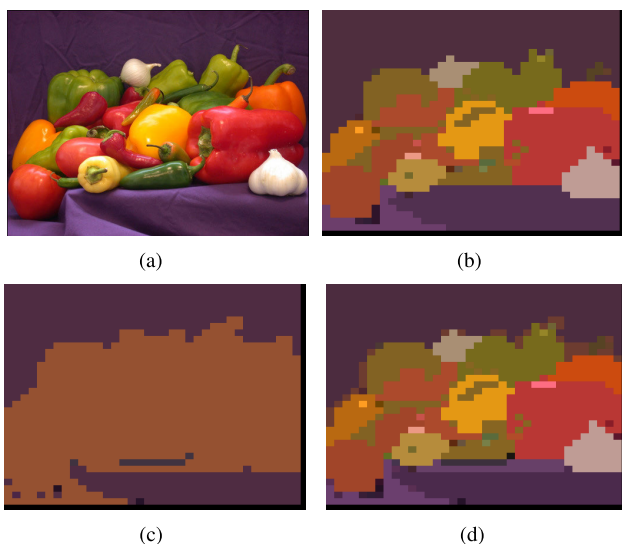


FIGURE 2. Application of the proposed segmentation to a simple input image (513 × 383): (a) original image, (b) Thread 1: ADP + GDD clustering, (c) Thread 2: mean-HSV + GDD clustering, (d) the final image is obtained by means of intersecting the blocks coming from the threads.

TABLE 1. Cluster based and semantic segmentation comparison results with proposed segmentation methods using Purity, Conditional Purity, NMI, F-Score and Intersection over Union (IoU) metrics.

Method (Segment Count)	C-Purity	Purity	NMI	F-Score		Intersection of Union	
				F-1	F-2	Score	Mean
Image 253027 (Zebra)							
MeanHSV-GDD (6)	55.9	69.8	20.8	54.4	56.0	28.2	3.3
ADP-GDD (3)	68.3	98.0	16.6	66.8	56.7	34.5	2.3
Resulting Segmentation (8)	55.8	69.7	20.9	54.4	56.0	28.2	3.3
Kmeans color (18)	12.2	12.4	5.3	14.8	27.9	7.0	2.5
Kmeans spatial (18)	19.8	20.4	24.0	16.2	30.4	11.9	4.8
MeanShift color (2)	72.7	96.2	2.0	71.0	60.8	36.4	3.1
MeanShift spatial (14)	31.7	33.2	18.5	28.1	42.5	18.0	5.0
MeanShift spatial (12)	32.0	34.0	18.6	28.1	42.0	17.0	4.9
Model 1 (ADE20k)	64.6	79.4	12.5	63.4	65.0	32.6	4.0
Model 2 (Cityscapes)	51.1	59.4	12.3	45.5	53.5	26.2	5.1
Model 3 (PascalVOC2012)	70.2	100.0	0.0	68.5	57.6	35.1	2.3
Model 4 (MobileNetV2)	70.2	100.0	0.0	68.5	57.6	35.1	2.3
Image 100080 (Bear)							
MeanHSV-GDD (11)	77.2	79.6	56.3	72.6	73.7	40.7	18.9
ADP-GDD (17)	68.7	91.4	67.2	67.7	59.8	35.3	19.7
Resulting Segmentation (25)	76.7	78.2	59.3	75.3	79.0	41.1	22.1
Kmeans color (12)	47.1	48.4	47.8	45.8	57.9	24.4	14.2
Kmeans spatial (12)	33.4	34.9	52.5	36.2	51.5	21.9	10.2
MeanShift color (2)	58.2	89.2	25.3	55.0	45.1	29.1	6.0
MeanShift spatial (12)	51.4	54.4	43.2	50.1	54.4	27.2	11.8
Model 1 (ADE20k)	51.2	69.2	48.7	48.3	47.4	26.7	9.8
Model 2 (Cityscapes)	70.0	88.2	42.4	67.9	64.1	35.6	11.0
Model 3 (PascalVOC2012)	40.7	100.0	0.0	40.9	30.1	20.3	2.4
Model 4 (MobileNetV2)	57.4	96.1	11.8	51.2	40.3	28.7	6.4
Image 145086 (Parade)							
MeanHSV-GDD (5)	69.8	93.9	39.5	76.9	71.1	34.9	5.4
ADP-GDD (30)	75.7	84.5	40.8	81.5	83.6	38.2	14.0
Resulting Segmentation (42)	74.2	82.3	40.9	81.3	86.2	38.3	15.7
Kmeans color (28)	27.9	32.5	25.3	27.2	42.8	15.2	8.7
Kmeans spatial (28)	35.2	39.7	38.1	31.4	49.8	19.8	12.7
MeanShift color (4)	52.3	93.1	13.7	58.5	47.7	26.1	4.7
MeanShift spatial (20)	55.3	66.7	38.1	61.3	70.2	28.7	11.8
MeanShift spatial (19)	59.1	70.3	37.0	63.3	71.3	30.7	12.3
Model 1 (ADE20k)	65.0	89.3	33.2	65.3	58.7	33.2	7.2
Model 2 (Cityscapes)	47.4	68.7	26.2	44.1	42.4	25.0	4.9
Model 3 (PascalVOC2012)	36.2	98.0	5.4	35.7	25.8	18.2	2.5
Model 4 (MobileNetV2)	36.2	97.0	6.4	35.4	25.7	18.1	3.2
Image 101087 (Tribal)							
MeanHSV-GDD (9)	55.0	85.2	38.7	54.1	45.8	27.5	3.8
ADP-GDD (28)	56.4	77.0	46.1	63.9	60.4	28.4	6.7
Resulting Segmentation (43)	55.1	74.1	45.4	63.4	62.2	28.4	7.8
Kmeans color (32)	41.2	44.8	34.4	52.0	62.5	21.6	6.5
Kmeans spatial (32)	36.5	37.4	44.0	30.7	48.1	20.4	12.8
MeanShift color (4)	55.8	81.6	32.7	53.2	43.8	27.9	3.5
MeanShift spatial (23)	37.7	52.8	44.6	41.9	49.7	19.6	8.7
MeanShift spatial (24)	39.9	55.2	44.7	42.5	50.2	20.8	8.9
Model 1 (ADE20k)	63.2	85.8	47.7	63.8	56.0	32.0	8.8
Model 2 (Cityscapes)	58.2	81.9	45.4	67.9	61.5	29.6	5.7
Model 3 (PascalVOC2012)	39.8	92.8	4.9	31.1	22.3	20.0	2.0
Model 4 (MobileNetV2)	41.6	94.2	4.2	32.4	23.3	20.8	2.1

TABLE 1. (Continued.) Cluster based and semantic segmentation comparison results with proposed segmentation methods using Purity, Conditional Purity, NMI, F-Score and Intersection over Union (IoU) metrics.

Method (Segment Count)	C-Purity	Purity	NMI	F-Score		Intersection of Union	
				F-1	F-2	Score	Mean
Image 170057 (Soldiers)							
MeanHSV-GDD (6)	25.5	75.7	10.2	27.8	20.5	12.8	1.8
ADP-GDD (8)	24.6	96.1	7.4	25.8	17.9	12.3	3.0
Resulting Segmentation (20)	26.1	74.8	11.5	28.0	20.7	13.1	4.1
Kmeans color (35)	13.8	14.5	10.6	13.3	21.0	07.5	3.8
Kmeans spatial (35)	27.0	27.9	42.2	24.3	39.6	15.8	8.4
MeanShift color (1)	23.5	100.0	0.0	24.8	17.1	11.8	0.5
MeanShift spatial (12)	45.1	57.8	30.4	42.9	42.4	23.0	6.1
MeanShift spatial (13)	43.7	59.6	30.1	42.5	41.6	22.3	5.8
Model 1 (ADE20k)	38.0	65.9	22.6	35.1	31.0	19.3	4.6
Model 2 (Cityscapes)	44.6	82.1	9.8	40.6	31.8	22.4	3.4
Model 3 (PascalVOC2012)	29.3	95.3	7.1	29.8	21.0	14.7	2.7
Model 4 (MobileNetV2)	32.0	97.5	6.5	31.4	22.3	16.0	2.7
Image 208001 (Mushroom)							
MeanHSV-GDD (5)	24.3	97.4	0.9	25.0	17.4	12.2	1.2
ADP-GDD (9)	32.4	95.6	7.8	30.5	21.7	16.2	2.7
Resulting Segmentation (13)	32.1	94.9	8.3	30.5	21.7	16.1	2.8
Kmeans color (25)	17.2	20.1	15.2	14.6	21.4	09.2	5.3
Kmeans spatial (25)	36.3	38.7	41.8	33.0	48.2	20.1	13.2
MeanShift color (2)	27.8	96.2	3.7	26.1	18.2	13.9	1.9
MeanShift spatial (15)	50.7	57.1	41.1	44.7	52.0	25.8	11.7
Model 1 (ADE20k)	33.0	72.5	16.3	32.9	26.8	16.7	3.1
Model 2 (Cityscapes)	35.1	82.3	18.4	35.4	26.4	17.7	5.2
Model 3 (PascalVOC2012)	35.8	85.3	23.2	31.5	23.7	17.9	2.0
Model 4 (MobileNetV2)	31.1	97.3	8.2	27.6	19.3	15.5	2.5
Image 227092 (Vase)							
MeanHSV-GDD (5)	72.0	94.8	12.7	69.3	60.5	36.0	10.4
ADP-GDD (13)	88.5	94.0	35.6	86.3	83.6	44.4	19.8
Resulting Segmentation (17)	87.8	91.9	35.1	86.6	85.7	44.1	22.1
Kmeans color (10)	37.2	38.4	28.8	43.6	60.4	20.6	11.2
Kmeans spatial (10)	34.3	35.8	47.8	33.2	47.3	18.0	11.8
MeanShift color (2)	51.9	91.2	26.9	58.1	48.5	26.0	7.1
MeanShift spatial (10)	44.2	47.9	44.6	47.4	63.1	23.1	12.0
Model 1 (ADE20k)	54.4	91.0	45.1	56.1	47.2	28.0	8.8
Model 2 (Cityscapes)	44.2	94.0	13.9	49.6	38.5	22.1	5.5
Model 3 (PascalVOC2012)	38.6	100.0	0.0	47.3	35.9	19.3	2.8
Model 4 (MobileNetV2)	47.8	85.8	6.9	44.3	35.4	23.9	5.3
Image 241004 (Rocks)							
MeanHSV-GDD (7)	59.3	90.5	39.0	49.1	39.2	29.6	12.2
ADP-GDD (14)	53.0	93.6	39.5	47.9	37.3	26.8	12.5
Resulting Segmentation (25)	60.9	88.7	40.7	52.4	42.9	30.9	16.9
Kmeans color (17)	54.9	59.1	31.9	59.0	62.5	28.5	18.3
Kmeans spatial (17)	60.2	62.2	40.8	57.3	66.6	32.6	25.2
MeanShift color (4)	55.0	95.2	34.6	46.8	36.2	27.5	8.9
MeanShift spatial (9)	69.0	89.0	38.6	70.6	65.4	34.5	17.7
Model 1 (ADE20k)	53.3	72.2	33.2	52.0	46.3	27.1	12.0
Model 2 (Cityscapes)	36.3	78.0	23.5	27.2	20.0	18.3	8.1
Model 3 (PascalVOC2012)	17.6	100.0	0.0	19.6	13.2	8.8	0.9
Model 4 (MobileNetV2)	17.6	100.0	0.0	19.6	13.2	8.8	0.9
Image 374067 (Wall)							
MeanHSV-GDD (9)	73.3	89.1	41.7	70.1	65.1	36.9	18.3

TABLE 1. (Continued.) Cluster based and semantic segmentation comparison results with proposed segmentation methods using Purity, Conditional Purity, NMI, F-Score and Intersection over Union (IoU) metrics.

Method (Segment Count)	C-Purity	Purity	NMI	F-Score		Intersection of Union	
				F-1	F-2	Score	Mean
ADP-GDD (14)	77.1	93.2	45.0	73.8	66.8	38.8	19.8
Resulting Segmentation (23)	72.3	87.5	42.3	70.8	67.0	36.6	20.1
Kmeans color (10)	49.5	49.5	29.2	45.4	55.3	24.8	15.5
Kmeans spatial (10)	54.3	54.7	44.9	56.0	71.7	31.4	18.1
MeanShift color (3)	67.0	94.3	35.9	60.2	50.1	33.5	12.5
MeanShift spatial (13)	65.9	66.1	42.6	64.3	75.0	35.3	20.3
Model1 (ADE20k)	56.5	76.5	39.2	59.2	55.2	30.9	18.2
Model2 (Cityscapes)	49.8	94.7	40.2	49.4	38.3	25.0	11.2
Model3 (PascalVOC2012)	31.7	100.0	0.0	37.9	27.6	15.8	2.4
Model4 (MobileNetV2)	31.7	99.8	0.3	37.8	27.6	15.9	3.0
Image 296059 (Elephants)							
MeanHSV-GDD (13)	44.7	87.1	30.3	42.6	33.2	22.4	5.0
ADP-GDD (31)	45.0	86.1	27.9	35.8	26.7	22.8	9.8
Resulting Segmentation (45)	48.6	78.8	34.4	49.8	41.5	24.7	11.0
Kmeans color (27)	21.1	22.5	21.0	24.5	33.0	10.8	6.8
Kmeans spatial (27)	35.0	40.2	42.1	34.0	47.7	20.7	12.0
MeanShift color (2)	38.4	99.5	18.7	30.6	21.6	19.2	2.5
MeanShift spatial (10)	54.7	71.1	34.5	49.5	46.0	27.9	9.5
MeanShift spatial (11)	54.4	71.0	35.7	49.7	46.7	27.7	9.5
Model 1 (ADE20k)	48.4	63.2	30.3	46.7	43.8	24.7	6.9
Model 2 (Cityscapes)	30.4	72.4	10.2	24.3	17.8	15.4	3.2
Model 3 (PascalVOC2012)	20.5	100.0	0.0	21.7	14.8	10.3	0.6
Model 4 (MobileNetV2)	20.5	100.0	0.0	21.7	14.8	10.3	0.6
Image 299091 (Pyramid)							
MeanHSV-GDD (10)	48.2	91.9	28.0	42.5	32.5	24.1	9.3
ADP-GDD (12)	47.0	96.2	28.1	41.7	31.3	23.5	9.2
Resulting Segmentation (23)	48.1	91.4	28.9	42.4	32.4	24.3	10.8
Kmeans color (11)	42.6	47.3	28.8	43.8	47.3	21.8	16.0
Kmeans spatial (11)	54.0	55.9	40.5	50.3	57.9	29.8	23.6
MeanShift color (1)	24.6	100.0	0.0	26.8	18.6	12.3	1.8
MeanShift spatial (9)	65.1	75.2	37.5	65.8	66.2	33.4	22.7
Model 1 (ADE20k)	43.5	73.5	31.8	40.2	32.0	23.4	11.5
Model 2 (Cityscapes)	41.5	72.3	24.5	37.9	30.9	20.9	10.6
Model 3 (PascalVOC2012)	24.6	100.0	0.0	26.8	18.6	12.3	1.8
Model 4 (MobileNetV2)	24.6	100.0	0.0	26.8	18.6	12.3	1.8

where $\Omega = \{\omega_1, \omega_2, \dots, \omega_K\}$ is the set of segments and $\mathbb{C} = \{c_1, c_2, \dots, c_J\}$ is the set of classes. Purity normally produces a number between 0 and 1, but a factor of 100 is added to see the results as percentage. Detailed information about purity, NMI and F-measure is given in the reference [36]. In the purity metric, a segment can be assigned to more than one class as long as $\omega_k \cap c_j$ is maximum, while in conditional purity metric, segments can only be assigned to one class.

V. RESULTS AND DISCUSSION

Figure 3 shows segmentation outputs of the rocks image obtained by using various methods. In all comparative results,

it should be noted that output of coarse segmentation is always low-resolution where mosaic (pixellated) output is caused by resolution upsampling to match the output resolution of other methods. The challenging aspect of this image in terms of segmentation tools is the accurate detection of objects among green tints. Shading and light also make the problem difficult. K-Means loses the real object because it finds too many segments and fails in this regard. Although meanshift can find dominant segments, it is affected by light changes. Similarly, Model 1 in Figure 3.f finds many segments, however, faulty segmentation is observed where the light changes occurs.

Metrics can also be misleading sometimes. For example, the Purity metric showed %100 successful for the outputs of

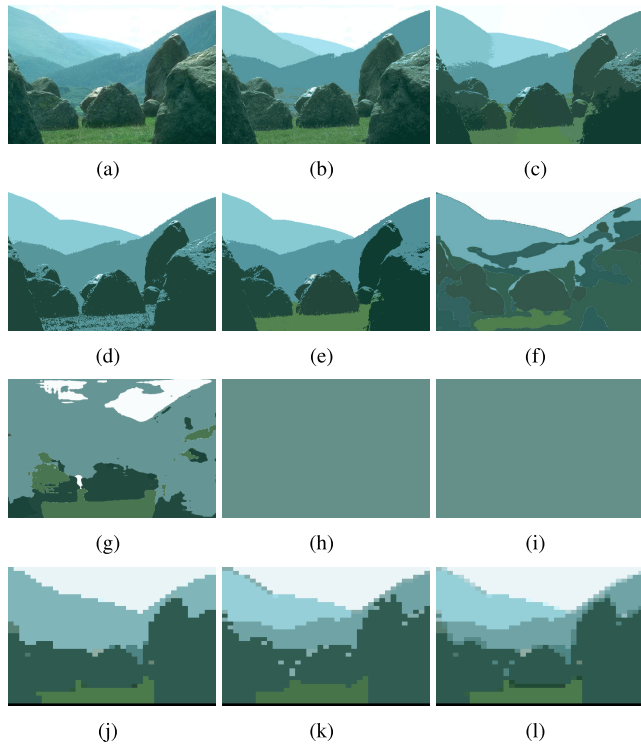


FIGURE 3. Segmentation of the rocks image (204×153) by different algorithms and proposed method: (a) original image, (b) k-means color segmentation, (c) k-means spatial segmentation, (d) meanshift color segmentation, (e) meanshift spatial segmentation, (f) PSPnet segmentation trained with ADE 20K dataset (model 1), (g) PSPnet trained with Cityscapes dataset (model 2), (h) PSPnet trained with Pascal VOC (model 3), (i) Deeplabv3 mobilenetv2 trained with Pascal VOC (model 4), (j) ADP-GDD (thread-1) segmentation, (k) meanHSV-GDD (thread-2) segmentation, (l) proposed segmentation result.

Model 3 and Model 4 in Figure 3.h-i. However, the algorithms did not actually perform an accurate segmentation.

As it can be seen from Figure 3, the rocks and the mountain segments are not correctly segmented by most of the methods except the proposed algorithm. The new method connects regions with their similar brightness differences and gradient color changes. Even though left hand side of the middle rock is over-segmented, rock objects correctly differentiated in general. GDD-based methods, different from other algorithms generally combines smooth transitions between pixels (segments are obtained), and thus large multi-area segments can be clearly distinguished. For example, in Figure 3, the rocks are segmented as a whole rather than separately. In spatial meanshift segmentation however, more crisp segments can be seen, but the rock segments are divided and fall short at purity side. Also, rock segments are divided at both sides in meanshift due to brightness change. With the downscaling approach, proposed algorithm gives more satisfactory results.

Color and space information of a pixel are not independent from each other. If color-only information is considered for segmentation by using any clustering algorithm, the results may be over-segmented. Colors are usually not evenly distributed over a region because of the light conditions as

well as the texture. For example, if natural segments are small and scattered in the image within a close location, they would form one big segment in the end. Keeping these facts in mind, feeding only color information to a clustering algorithm for segmentation inherently causes errors because most of the clustering methods use Euclidean distance to determine the relations.

The texture composition of the vase and the light create challenges for color segmentation algorithms. In comparative tests, the semantic segmentation methods did not achieve the desired success for the vase-227092 data as a general segmentation application. However, the object is segmented much better using the proposed approach compared to the other algorithms because of cumulative and connective behavior of GDD clustering (see Figure 4).

In our study, textured areas are not specifically processed. When GDD clustering algorithm is applied to HSV color space, even distant points are segmented together as long as they have a connection. However, due to this distance the points some pixels may also be included to other regions, causing over-segmentation. For these type of cases, texture information and/or salient region detection methods can be developed at future studies to enhance the success rates.

At another point, color and spatial information are not generally linearly related, and most of the segmentation approaches suffer from this property. As multivariate data of independent information spaces should not be concatenated directly, relation between two data-spaces can be studied to further improve the results. Especially, low saturation and low value pixels become hard to determine due to this dependency and nature of colors.

In Figure 5 (mushroom example), when HSV color space is analyzed it can be seen that the colors are mixed and hard to separate in pixel level. So, spatial information helps to locate dense color regions within high pixel areas on segments. GDD clustering can locate these highly dense color regions. In current version of the proposed segmentation, spatial information loosely included to color which is not normalized or scaled according to resolution.

According to results in Table 1, meanshift-spatial method produces the best results in general for mushroom experiment, however the object is divided into unnecessary partitions (see Figure 5.f). On the other hand, the proposed method differentiates foreground (mushroom) and background segments with small artifacts at the bottom left corner.

Figure 6 shows segmentation outputs for some other images in the database. As it can be seen from the figures, the proposed algorithm produces promising segmentation results comparing the other well-known methods.

During the study it has been observed that the algorithm becomes short on separating the regions with low contrast and low value color regions which causes over-segmentation at shadow of non-chromatic regions. Another weak point of GDD is that if two similar color regions have connection to each other at any point, GDD unites them into one segment because of similarity criteria of clustering technique.

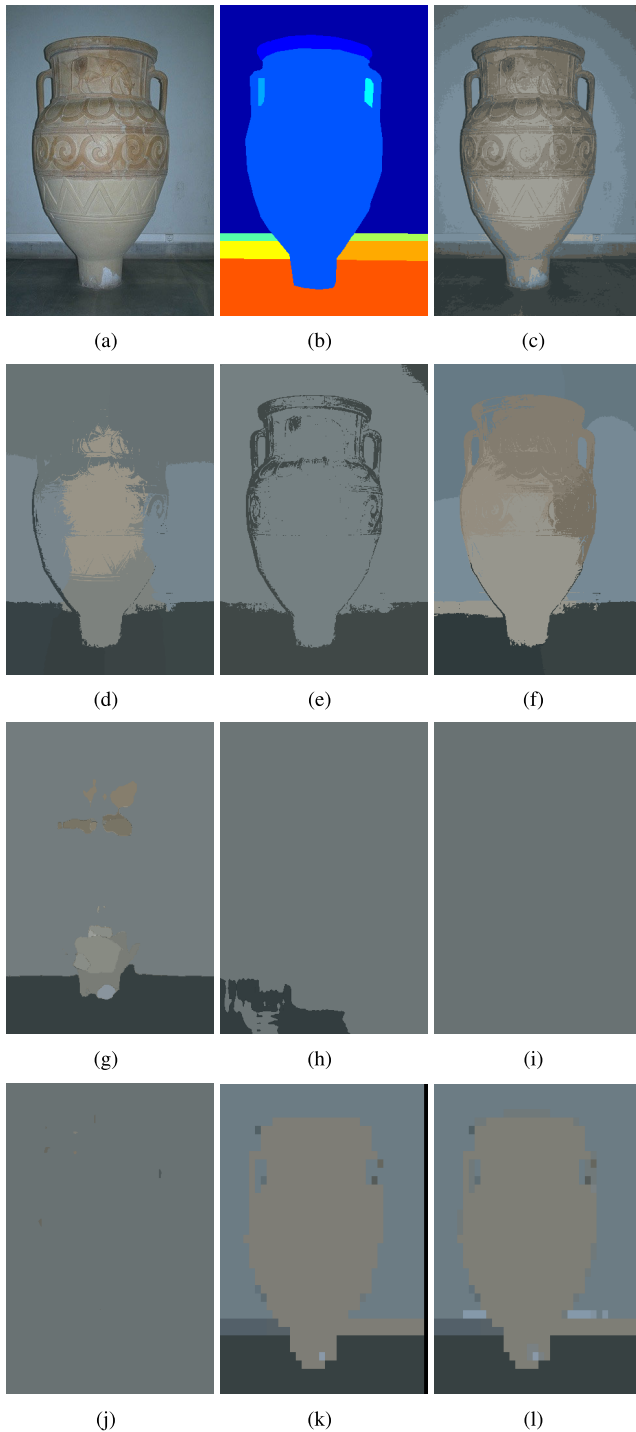


FIGURE 4. Segmentation of the vase image (321×481) by different algorithms and proposed method: (a) original image, (b) ground truth, (c) k-means color segmentation, (d) k-means spatial segmentation, (e) meanshift color segmentation, (f) meanshift spatial segmentation, (g) PSPnet segmentation trained with ADE 20K dataset (model 1), (h) PSPnet trained with Cityscapes dataset (model 2), (i) PSPnet trained with Pascal VOC (model 3), (j) Deeplabv3 mobilenetv2 trained with Pascal VOC (model 4), (k) ADP-GDD (thread-1) segmentation, (l) proposed segmentation result.

This study has an advantage on general segmentation concept over size based color regions, where other clustering based well-known methods fails. As an example for size

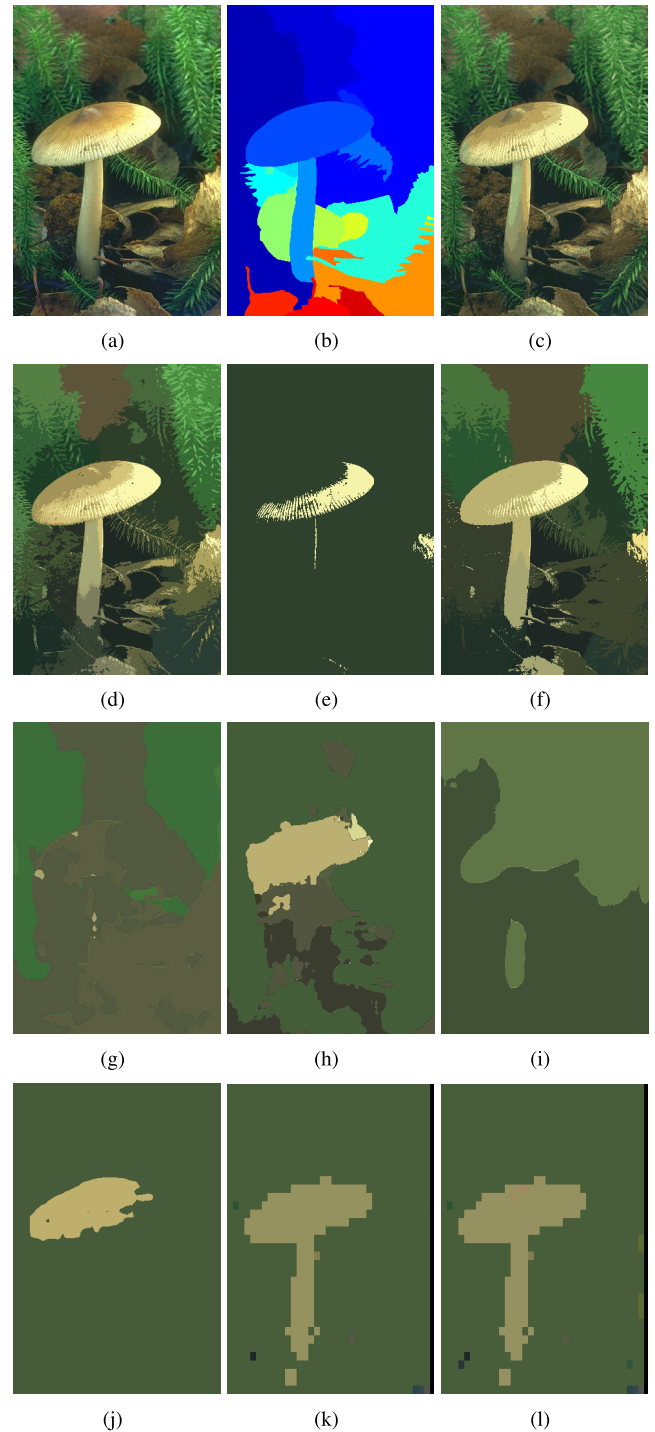


FIGURE 5. Segmentation of the mushroom image (321×481) by different algorithms and proposed method: (a) original image, (b) ground truth, (c) k-means color segmentation, (d) k-means spatial segmentation, (e) meanshift color segmentation, (f) meanshift spatial segmentation, (g) PSPnet segmentation trained with ADE 20K dataset (model 1), (h) PSPnet trained with Cityscapes dataset (model 2), (i) PSPnet trained with Pascal VOC (model 3), (j) Deeplabv3 mobilenetv2 trained with Pascal VOC (model 4), (k) ADP-GDD (thread-1) segmentation, (l) proposed segmentation result.

based color segmentation, when we see a human from a far distance, we are only be able to see a general shape and may understand that it is a human. However, when the

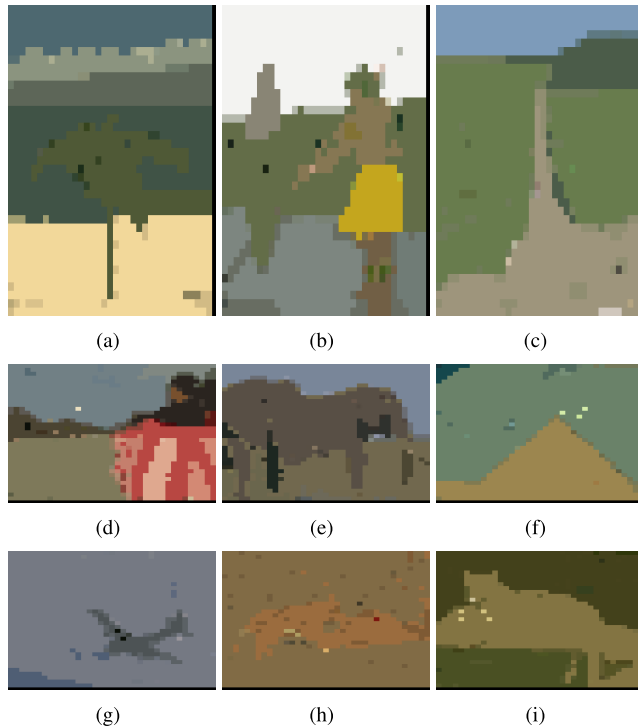


FIGURE 6. Segmentation outputs of the proposed algorithm: (a) Palm tree (46076), (b) Tribal (101087), (c) Wall (374067), (d) Parade (145086), (e) Elephant (296059), (f) Pyramid (299091), (g) Plane (3096), (h) Tiger-1 (187039), (i) Tiger-2 (160068). The first three images have (321 × 481) pixel size, and the rest have (481 × 321) pixel size.

person comes closer, we recognize the face features, clothes, hair styles and so on. So, level-of-detail in segmentation is related to distance which is directly related to the visible area. The proposed algorithm finds segments according to sizes of regions, colors, distances and brightness levels.

VI. CONCLUSION

In this study, a novel coarse segmentation algorithm based on color and spatial information with GDD clustering has been developed. The algorithm produces non-randomized stable outputs; i.e., the outputs do not change at different runs, and it does not require any parameter prior to run. Both global and spatial color similarities are used to enhance the results by using the GDD clustering method. Besides the use of the method in general color segmentation applications, the use of coarse segments will provide an advantage in region of interest operations.

In addition to the color and spatial properties, low resolution is also used effectively in the method, so that details are filtered while the fundamental attributes are generally preserved. This achieved by two different novel downscaling methods: ADP: Area Dominance Peak and mean-HSV. The method is compared with both classical unsupervised and pre-trained modern supervised approaches to see the performance. In comparative tests, successful results are obtained in determining coarse segment areas.

As future work, the performance of the algorithm can be optimized in thread-1 and composition section to decrease computation time. The success rates of the algorithm can also be improved for some specific applications by just incorporating different methods as new threads and implementing special functions in the composition section.

REFERENCES

- [1] J. Malik, S. Belongie, T. Leung, and J. Shi, "Contour and texture analysis for image segmentation," *Int. J. Comput. Vis.*, vol. 43, no. 1, pp. 7–27, Jun. 2001.
- [2] S. D. Yanowitz and A. M. Bruckstein, "A new method for image segmentation," *Comput. Vis., Graph., Image Process.*, vol. 46, no. 1, pp. 82–95, Apr. 1989.
- [3] L. Shafarenko, H. Petrou, and J. Kittler, "Histogram-based segmentation in a perceptually uniform color space," *IEEE Trans. Image Process.*, vol. 7, no. 9, pp. 1354–1358, Sep. 1998.
- [4] S. L. X. Fan, Z. Man, and R. Samur, "Edge based region growing: A new image segmentation method," in *Proc. ACM SIGGRAPH Int. Conf. Virtual Reality Continuum Appl. Ind. (VRCAI)*, New York, NY, USA, 2004, pp. 302–305.
- [5] A. Tremeau and N. Borel, "A region growing and merging algorithm to color segmentation," *Pattern Recognit.*, vol. 30, no. 7, pp. 1191–1203, Jul. 1997.
- [6] A. Mohanty, S. Rajkumar, Z. M. Mir, and P. Bardhan, "Analysis of color images using cluster based segmentation techniques," *Int. J. Comput. Appl.*, vol. 79, no. 2, pp. 42–47, Oct. 2013.
- [7] B. Peng, M. Simfukwe, and T. Li, "Region-based image segmentation evaluation via perceptual pooling strategies," *Mach. Vis. Appl.*, vol. 29, no. 3, pp. 477–488, Apr. 2018.
- [8] H. Zhao, J. Shi, X. Qi, X. Wang, and J. Jia, "Pyramid scene parsing network," in *Proc. IEEE Conf. Comput. Vis. Pattern Recognit. (CVPR)*, Jul. 2017, pp. 2881–2890.
- [9] M. Sandler, A. Howard, M. Zhu, A. Zhmoginov, and L.-C. Chen, "MobileNetV2: Inverted residuals and linear bottlenecks," in *Proc. IEEE/CVF Conf. Comput. Vis. Pattern Recognit.*, Jun. 2018, pp. 4510–4520.
- [10] L.-C. Chen, Y. Zhu, G. Papandreou, F. Schroff, and H. Adam, "Encoder-decoder with atrous separable convolution for semantic image segmentation," in *Proc. Eur. Conf. Comput. Vis. (ECCV)*, 2018, pp. 801–818.
- [11] L.-C. Chen, G. Papandreou, I. Kokkinos, K. Murphy, and A. L. Yuille, "DeepLab: Semantic image segmentation with deep convolutional nets, atrous convolution, and fully connected CRFs," *IEEE Trans. Pattern Anal. Mach. Intell.*, vol. 40, no. 4, pp. 834–848, Apr. 2018.
- [12] D. Comaniciu and P. Meer, "Robust analysis of feature spaces: Color image segmentation," in *Proc. Conf. Comput. Vis. Pattern Recognit. (CVPR)*, Washington, DC, USA: IEEE Computer Society, 1997, p. 750.
- [13] C. Kim, B.-J. You, M.-H. Jeong, and H. Kim, "Color segmentation robust to brightness variations by using B-spline curve modeling," *Pattern Recognit.*, vol. 41, no. 1, pp. 22–37, Jan. 2008.
- [14] M. Mignotte, "Segmentation by fusion of histogram-based K -means clusters in different color spaces," *IEEE Trans. Image Process.*, vol. 17, no. 5, pp. 780–787, May 2008.
- [15] C. Yang, R. Duraiswami, N. A. Gumerov, and L. Davis, "Improved fast gauss transform and efficient kernel density estimation," in *Proc. 9th IEEE Int. Conf. Comput. Vis.*, vol. 1, Oct. 2003, pp. 664–671.
- [16] E. Güngör and A. Özmen, "Distance and density based clustering algorithm using Gaussian kernel," *Expert Syst. Appl.*, vol. 69, pp. 10–20, Mar. 2017.
- [17] H. Caillol, W. Pieczynski, and A. Hillion, "Estimation of fuzzy Gaussian mixture and unsupervised statistical image segmentation," *IEEE Trans. Image Process.*, vol. 6, no. 3, pp. 425–440, Feb. 1997.
- [18] K. Fukunaga and L. Hostetler, "The estimation of the gradient of a density function, with applications in pattern recognition," *IEEE Trans. Inf. Theory*, vol. IT-21, no. 1, pp. 32–40, Jan. 1975.
- [19] J. Li, B. He, Y. Zhang, H. Chen, G. Li, and X. Tao, "Salient object detection based on meanshift filtering and fusion of colour information," *IET Image Process.*, vol. 9, no. 11, pp. 977–985, Nov. 2015.
- [20] C. Liu, Q. Zhang, G. Zhang, and A. Zhou, "Adaptive image segmentation by using mean-shift and evolutionary optimisation," *IET Image Process.*, vol. 8, no. 6, pp. 327–333, Jun. 2014.

- [21] A. K. Bhandari, A. Kumar, S. Chaudhary, and G. K. Singh, "A novel color image multilevel thresholding based segmentation using nature inspired optimization algorithms," *Expert Syst. Appl.*, vol. 63, pp. 112–133, Nov. 2016.
- [22] C. K. Chow and T. Kaneko, "Automatic boundary detection of the left ventricle from cineangiograms," *Comput. Biomed. Res.*, vol. 5, no. 4, pp. 388–410, Aug. 1972.
- [23] M. Huang, W. Yu, and D. Zhu, "An improved image segmentation algorithm based on the otsu method," in *Proc. SNPD*, T. Hochin and R. Y. Lee, Eds. Washington, DC, USA: IEEE Computer Society, 2012, pp. 135–139.
- [24] J. Canny, "A computational approach to edge detection," *IEEE Trans. Pattern Anal. Mach. Intell.*, vol. PAMI-8, no. 6, pp. 679–698, Nov. 1986.
- [25] A. Bleau and L. J. Leon, "Watershed-based segmentation and region merging," *Comput. Vis. Image Understand.*, vol. 77, no. 3, pp. 317–370, Mar. 2000.
- [26] A. Melouah, *Comparison of Automatic Seed Generation Methods for Breast Tumor Detection Using Region Growing Technique*. Cham, Switzerland: Springer, 2015, pp. 119–128.
- [27] F. Y. Shih and S. Cheng, "Automatic seeded region growing for color image segmentation," *Image Vis. Comput.*, vol. 23, no. 10, pp. 877–886, Sep. 2005.
- [28] J. Shi and J. Malik, "Normalized cuts and image segmentation," *IEEE Trans. Pattern Anal. Mach. Intell.*, vol. 22, no. 8, pp. 888–905, Aug. 2000.
- [29] A. Fahad and T. Morris, "A faster graph-based segmentation algorithm with statistical region merge," in *Advances in Visual Computing*. Berlin, Germany: Springer, 2006, pp. 286–293.
- [30] H. Vu and R. Olsson, "Automatic improvement of graph based image segmentation," in *Advances in Visual Computing*. Berlin, Germany: Springer, 2012, pp. 578–587.
- [31] J. C. Russ, *Image Processing Handbook*, 4th ed. Boca Raton, FL, USA: CRC Press, 2002.
- [32] *MATLAB Version 8.5.0 (R2015a)*, MathWorks, Natick, MA, USA, 2015.
- [33] D. Martin, C. Fowlkes, D. Tal, and J. Malik, "A database of human segmented natural images and its application to evaluating segmentation algorithms and measuring ecological statistics," in *Proc. 8th IEEE Int. Conf. Comput. Vis. (ICCV)*, vol. 2, Jul. 2001, pp. 416–423.
- [34] A. Asvadi, M. Karami-Mollaie, Y. Baleghi, and H. Seyyedi-Andi, "Improved object tracking using radial basis function neural networks," in *Proc. 7th Iranian Conf. Mach. Vis. Image Process. (MVIP)*, Nov. 2011, pp. 1–5.
- [35] W. Tao, H. Jin, and Y. Zhang, "Color image segmentation based on mean shift and normalized cuts," *IEEE Trans. Syst. Man, Cybern. B, Cybern.*, vol. 37, no. 5, pp. 1382–1389, Oct. 2007.
- [36] C. D. Manning, P. Raghavan, and H. Schütze, *Introduction to Information Retrieval*. New York, NY, USA: Cambridge Univ. Press, 2008.



EMRE GÜNGÖR received the Ph.D. degree from the Computer Engineering Department, Sakarya University, in 2018. He is currently working as an Assistant Professor with the Computer Engineering Department, Alanya Hamdullah Emin Pasa University. His current research interests include computer vision and clustering.



AHMET ÖZMEN (Member, IEEE) received the B.S. degree from the Electronics and Communication Engineering Department, Istanbul Technical University, Istanbul, Turkey, in 1987, and the M.S.E.E. and Ph.D. degrees from the Electrical Engineering Department, University of Kentucky, Lexington, USA, in 1996 and 2000, respectively. He is currently with the Software Engineering Department, Sakarya University. His main research interests include data processing and monitoring systems.

• • •